Examples of propagating and non-propagating singularities in thin shell theory

E. Sanchez – Palencia

**(Institut Jean Le Rond d'Alembert
Université Paris VI)**

Joint work with

F. Béchet (Lille I)

Y. V. Egorov (Toulouse III)

O. Millet (La Rochelle)

The shell equations involve a small parameter ε: the relative shell thickness, i.e. the ratio between the actual thickness of the shell and a characteristic length of the structure. In the Kirchhoff-Love framework as well as in the Mindlin one, the system of equations is elliptic for $\varepsilon > 0$ and the solution enjoys the classical smoothness properties predicted by the regularity theory. But the limit system obtained as ε tends to 0 is elliptic only if the middle surface is itself elliptic, i.e. if the principal curvatures have equal signs at any point.

Surface types

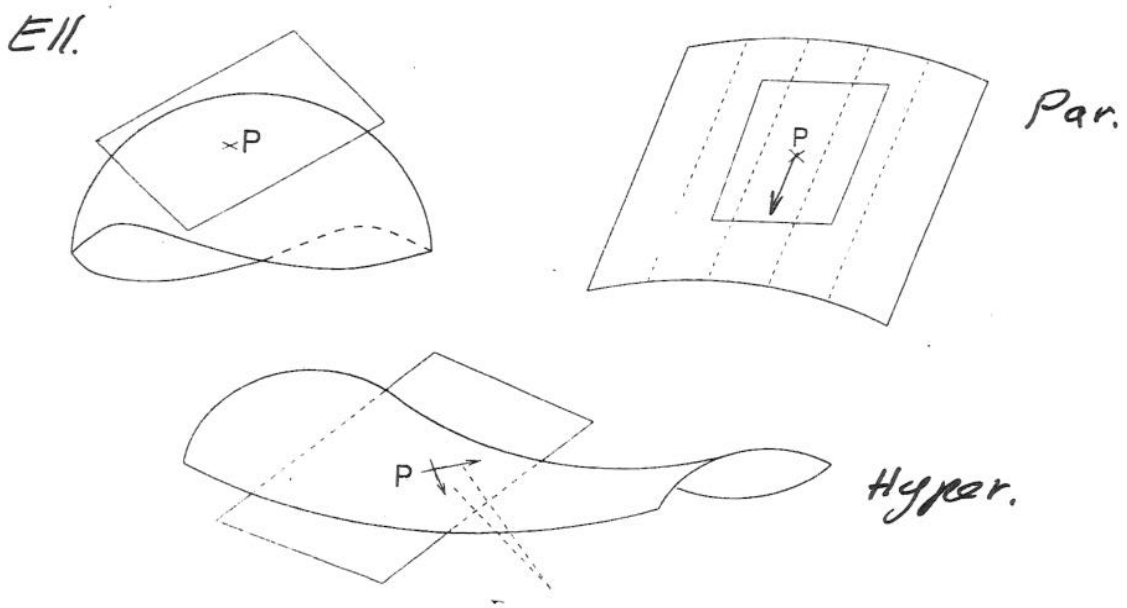

3. INHIBITED SHELLS. BOUNDARY LAYERS

= (geometrically rigid surfaces)

In any case, the limit solution as ε tends to zero is not very smooth, whereas u^ε with $\varepsilon > 0$ is smooth. Then, boundary layer phenomena appear, as we pointed out at the end of the previous section.

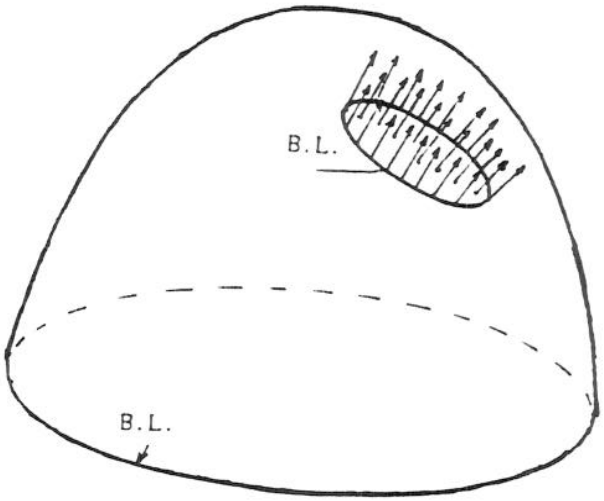

Figure 2

Our present knowledge of boundary layers (also called "edge effects" [13], [1]) is very incomplete, but we are giving here some indication which should be very useful for a good understanding of numerical computations. **The boundary (or internal) layers are regions with thickness tending to zero as ε tends to zero where the solution $\mathbf{u}^\varepsilon$ (or certain derivatives of $\mathbf{u}^\varepsilon$) have gradients tending to infinity as ε tends to zero.**

The *order of thickness of layers* (up to our present knowkledge) is

a) $\eta = O(\varepsilon^{1/2})$ along curves which are not characteristics,

b) $\eta = O(\varepsilon^{1/3})$ along curves which are simple characteristics (hyperbolic case),

c) $\eta = O(\varepsilon^{1/4})$ along curves which are double characteristics (parabolic case).

These boundary layers appear in the following situations (non-exhaustive list) :

1. along the boundaries of the surface S,
2. along the discontinuities of the loading $\mathbf{f}$,
3. along the curves where either the curvature or the tangent plane of the surface are not continuous, = Tr.9
4. along the characteristics issued from corner points of the boundary,
5. along the characteristics which are somewhere tangent to one of the previous curves.

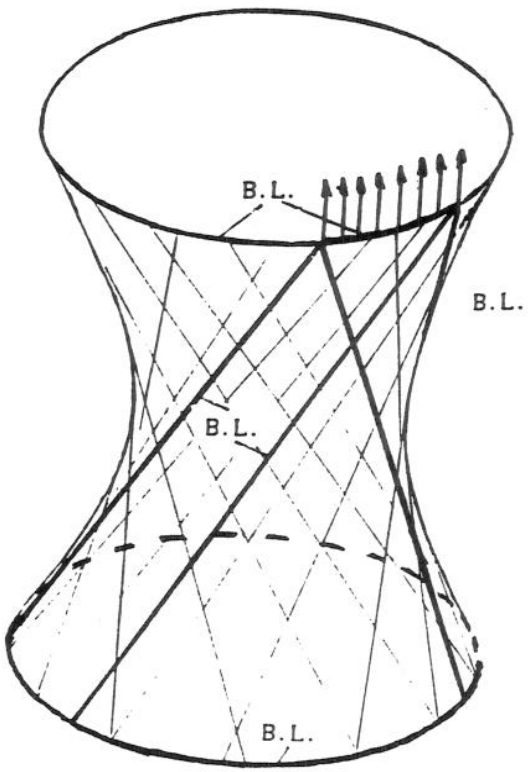

Figure 4

Let us illustrate this by a few examples. In figure 2

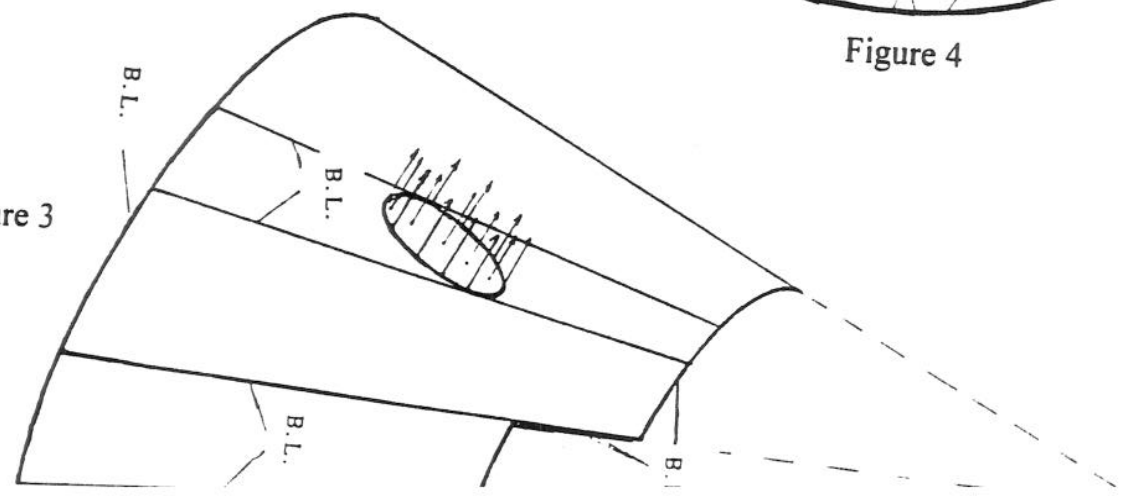

Figure 3

The elliptic sensitive case

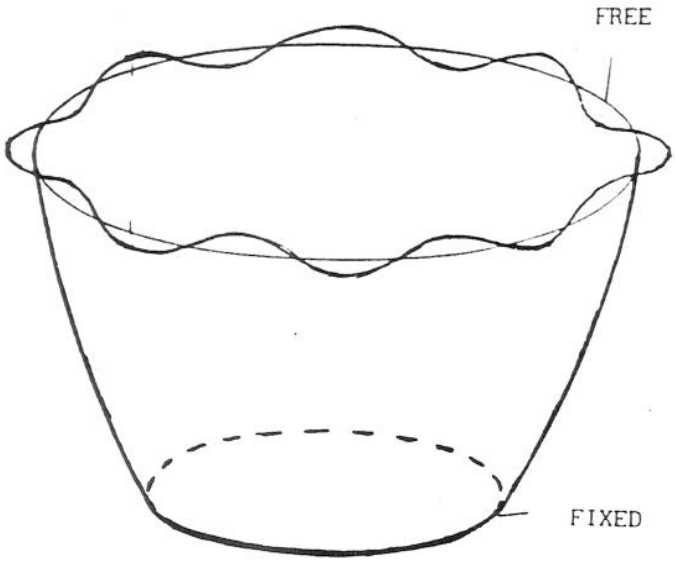

$$\mathbf{u}^{\varepsilon}(y^1, y^2) \approx \sin(y^1 / \ell(\varepsilon))\exp(y^2 / \ell(\varepsilon))$$

Coming back to the case of an elliptic middle surface fixed (or clamped) by a part of its boundary and free by the rest, above called "sensitive", strictly speaking it is geometrically rigid, but the corresponding "limit problem" is not well posed, as very small and even smooth loadings may generate very large solutions. In fact the mathematical structure of that problem keeps some relation with the Cauchy problem for elliptic systems.

Model Problem

We consider examples which are elliptic for $\varepsilon > 0$ and parabolic at the limit $\varepsilon = 0$.

$$\begin{cases} -\Delta u_1^\varepsilon + \partial_2 u_2^\varepsilon = f_1 \\ -\partial_2 u_1^\varepsilon + u_2^\varepsilon + \varepsilon^2 \left(\Delta^2 u_2^\varepsilon - \Delta u_2^\varepsilon + u_2^\varepsilon \right) = f_2 \end{cases}$$

$$-\Delta u_1 + \partial_2 u_2 = f_1,$$
$$-\partial_2 u_1 + u_2 = f_2.$$

Or

$$-\partial_1^2 u_1 = f_1 - \partial_2 f_2$$
$$u_2 = \partial_2 u_1 + f_2$$

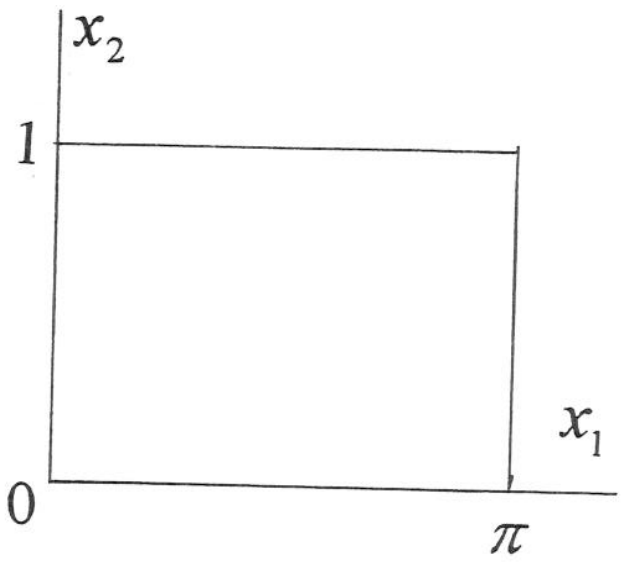

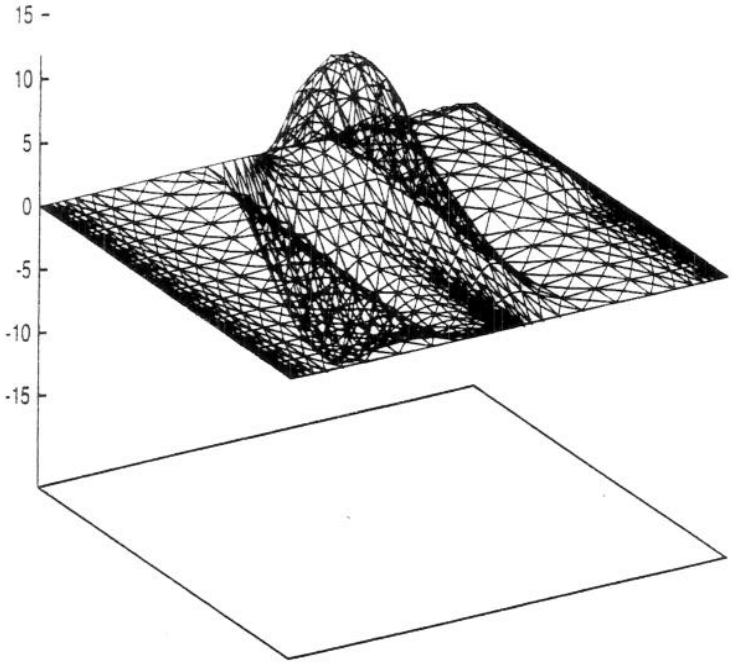

FIG. 9 – Three dimensional plot of U_2 for uniform unit square loading (Adapted mesh)

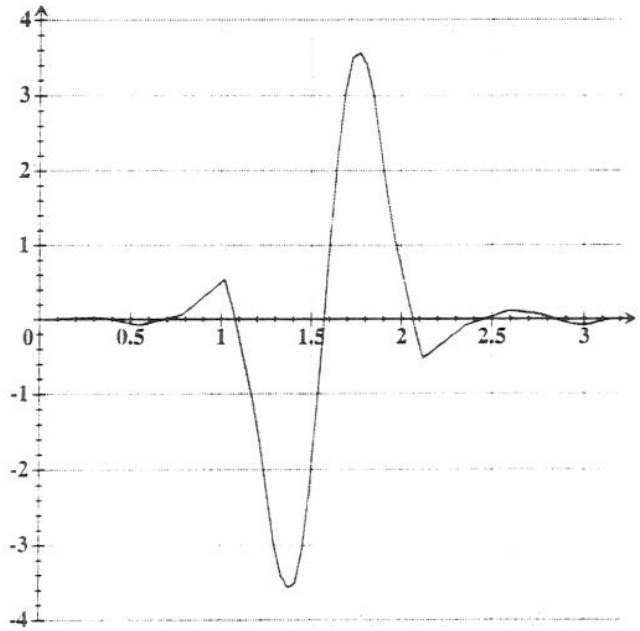

FIG. 10 – Graph of U_2 along the cross section $x=3\pi/4$

A model problem.

All the essential features of the above problems are present in the following model problem. Moreover, there are only two unknowns and only one system of characteristics (x_2 = Const).

$$\begin{cases} -\Delta u_1^\varepsilon + \partial_2 u_2^\varepsilon = f_1 \\ -\partial_2 u_1^\varepsilon + u_2^\varepsilon + \varepsilon^2 \left(\Delta^2 u_2^\varepsilon - \Delta u_2^\varepsilon + u_2^\varepsilon \right) = f_2 \end{cases}$$

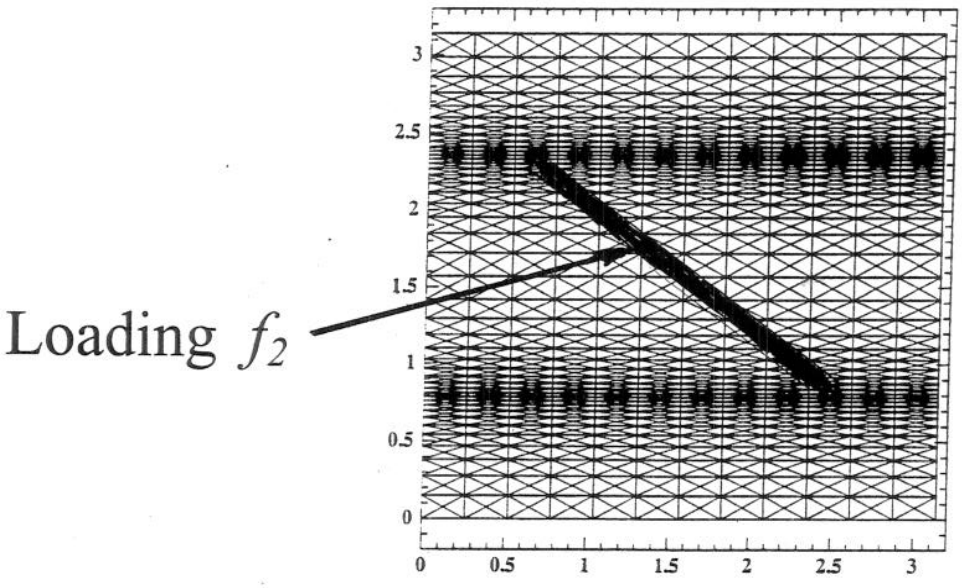

FIG. 3 – Adapted mesh for internal layers

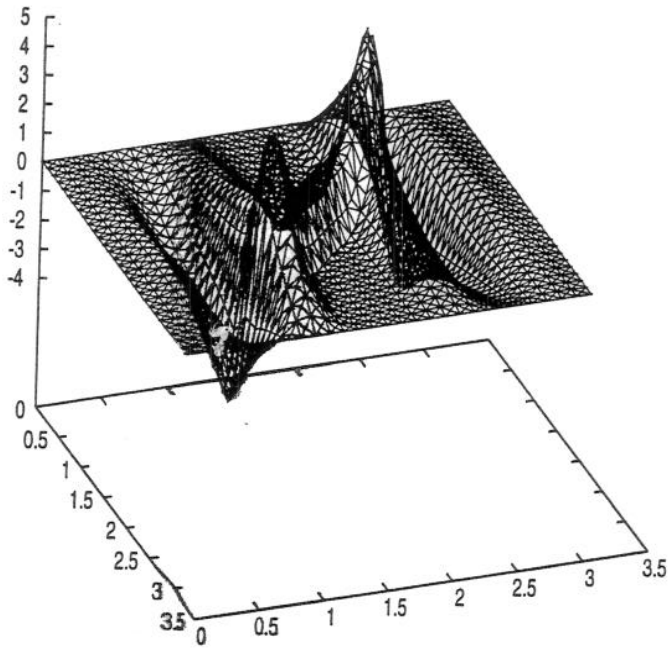

FIG. 11 – Three dimensional plot of U_2 for internal layer with propagation (Adapted mesh)

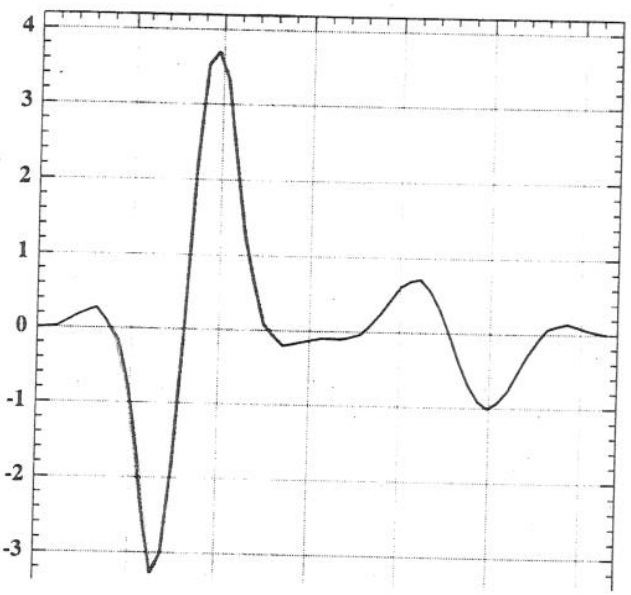

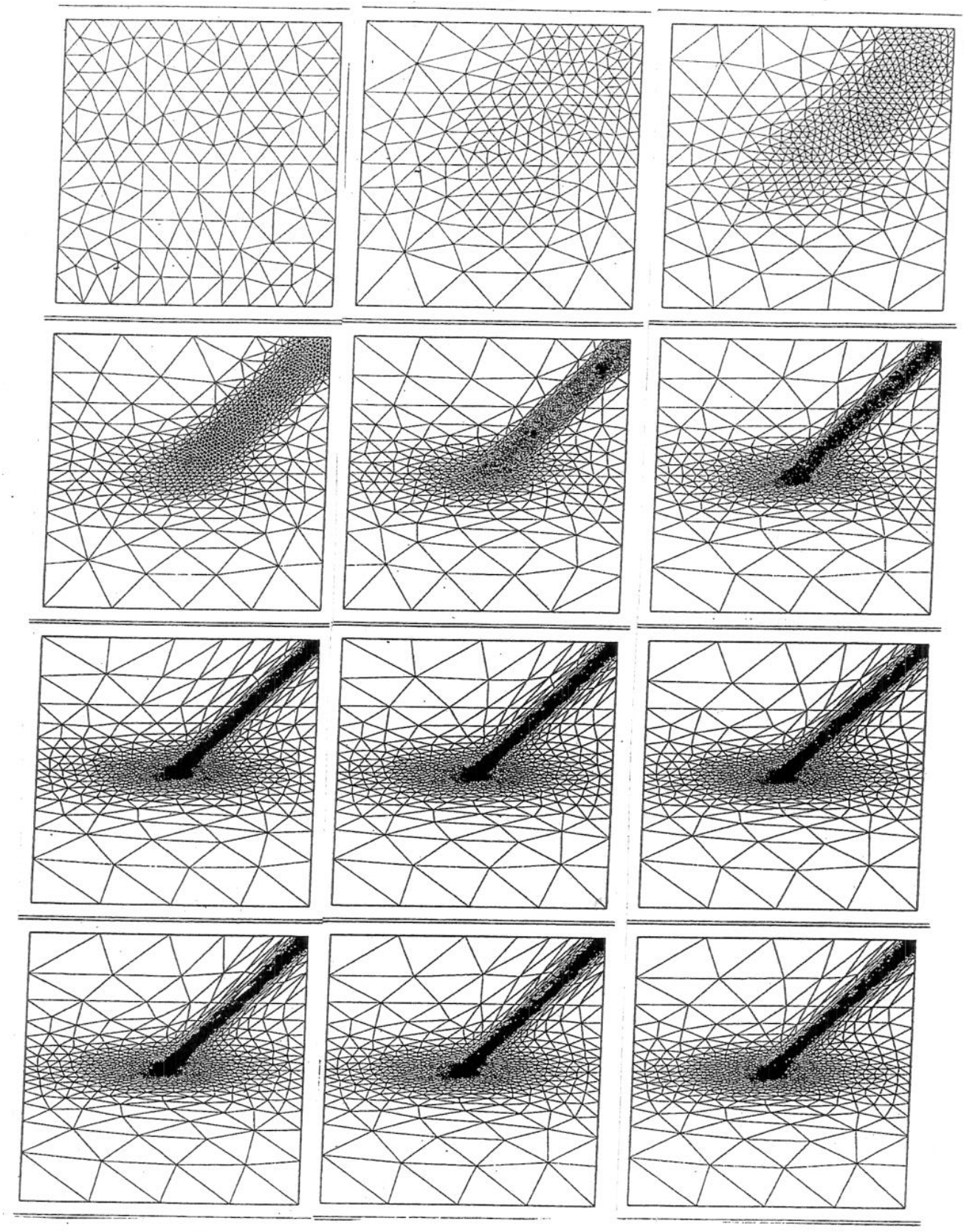

Iterations for the model problem with $\varepsilon = 10^{-4}$.
F E are P_1 and Zienkiewicz for u_1 and u_2 respectively.

b)

Asymptotic behaviour for rigid S (inhibited case)

The scaling is

$$\tilde{\mathbf{f}} = \delta\varepsilon\mathbf{f} \qquad (\mathbf{f} \text{ independent of } \varepsilon)$$
$$\tilde{\mathbf{v}} = \delta\mathbf{u}$$

Roughly speaking, the limit behaviour is given by the membrane state. In fact, the problem involves a *singular perturbation*, as the order of differentiation is lower in the limit problem. There appear *boundary layers* (both membrane and flexion terms are significant in the layers)

$$u^{\varepsilon} \to u \text{ (= solution of the membrane problem)}$$

in "very poor topologies" as u is "somewhat non - smooth".

The limit problem is (twice) of the type of the surface (elliptic, parabolic, hyperbolic).

$$-D_1 T^{11} - D_2 T^{12} = f^1$$
$$-D_1 T^{12} - D_2 T^{22} = f^2$$
$$-b_{11} T^{11} - 2b_{12} T^{12} - b_{22} T^{22} = f^3$$

$$\gamma_{11}(u) \equiv D_1 u_1 - b_{11} u_3 = C_{11\alpha\beta} T^{\alpha\beta}$$
$$\gamma_{22}(u) \equiv D_2 u_2 - b_{22} u_3 = C_{22\alpha\beta} T^{\alpha\beta}$$
$$\gamma_{12}(u) \equiv \frac{1}{2}(D_2 u_1 + D_2) - b_{12} u_3 = C_{12\alpha\chi} T^{\alpha\beta}$$

Each of the subsystems is of the type of the surface

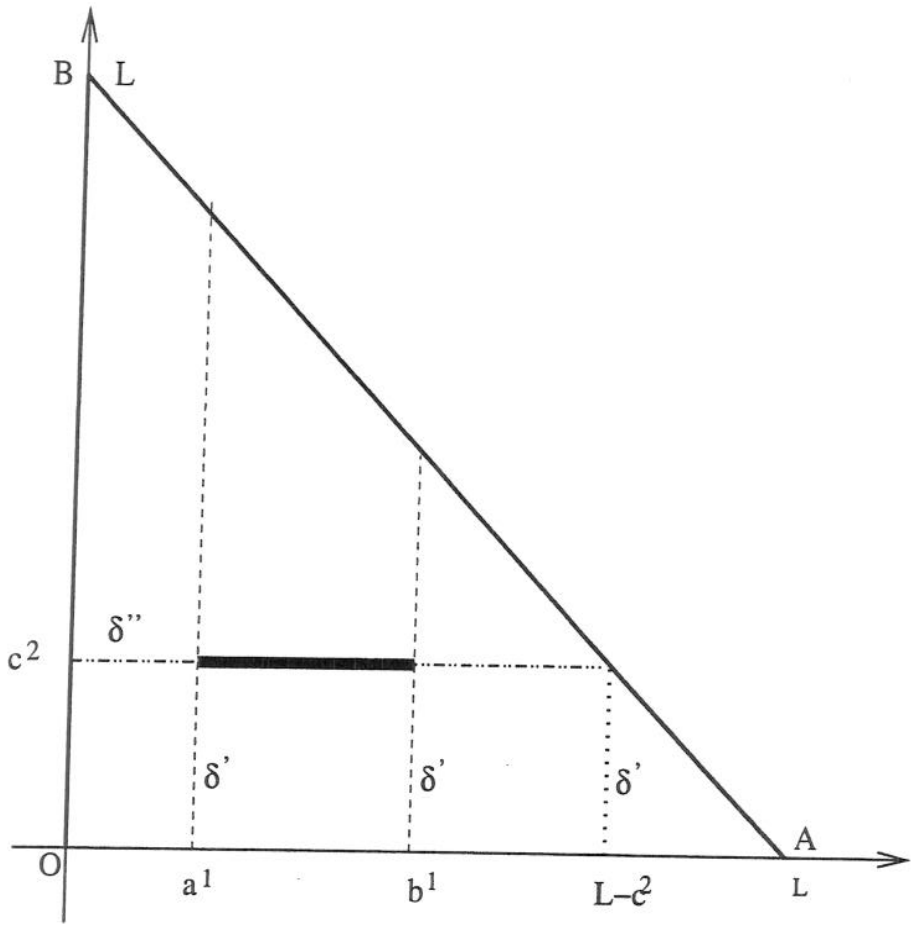

figure 3.1 : domain Ω in the first case of loading (3.2)
δ', δ'' indicate the type of singularity of u_3

Hyperbolic shell

The axes are taken in the direction of the characteristics.

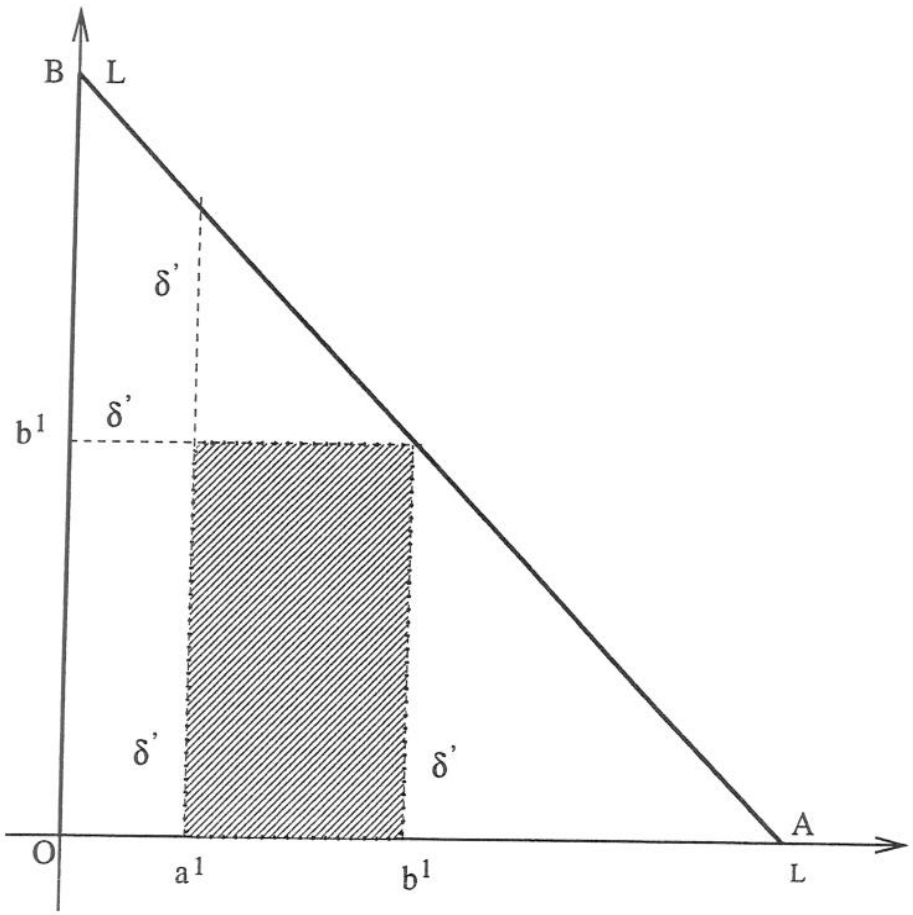

figure 3.2 : domain Ω in the second case of loading (3.26)
δ' indicates the type of singularity along the characteristics

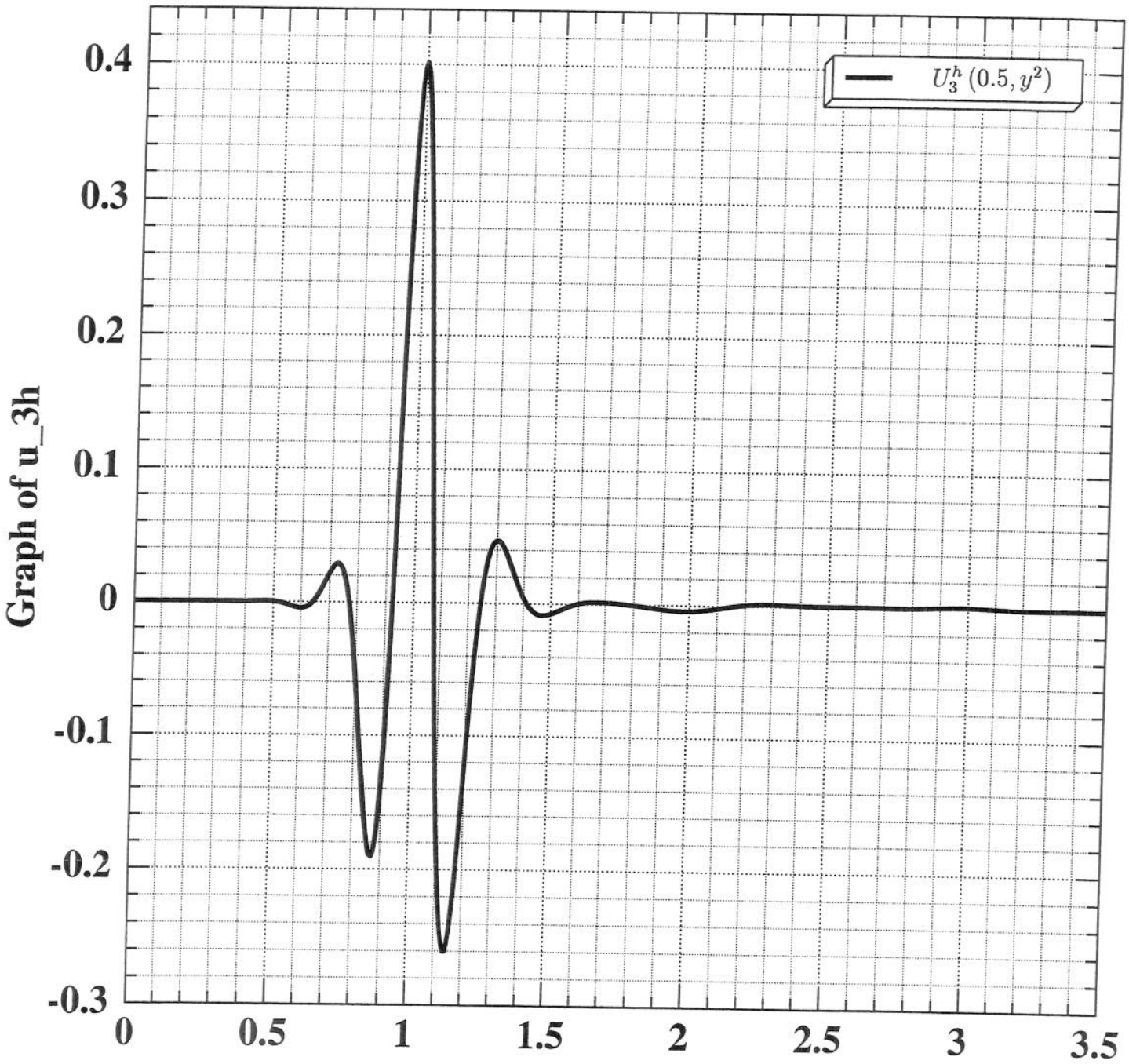

figure 4.1 : first example of loading, sect. 3.1. Plot of u_3 for $y^1 = 0.5$ exhibiting a propagated δ'' - like singularity at $y^2 = 1$.

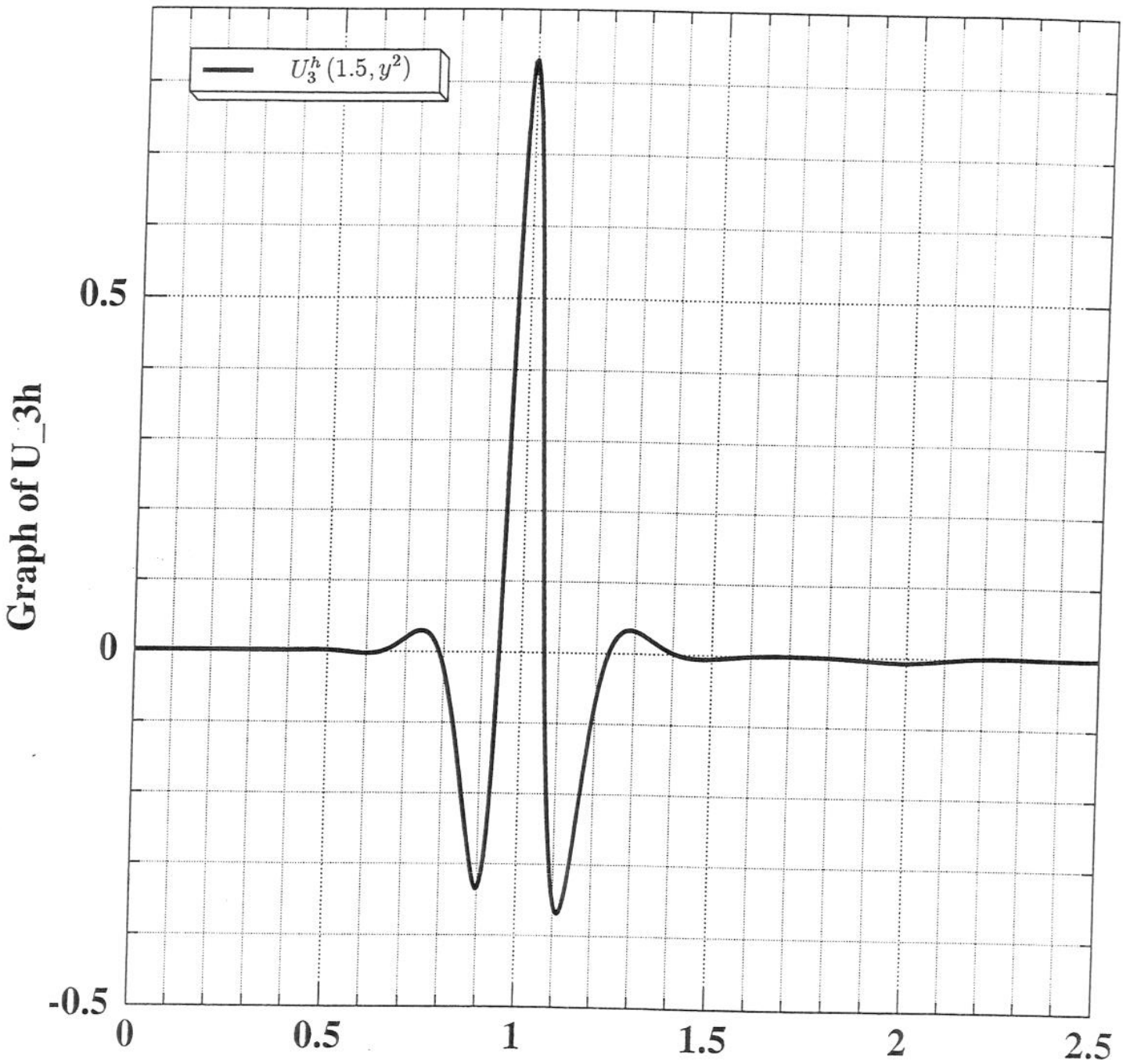

figure 4.2 : first example of loading, sect. 3.1 . Plot of u_3 for $y^1 = 1.5$ exhibiting a non - propagated singularity at $y^2 = 1$.

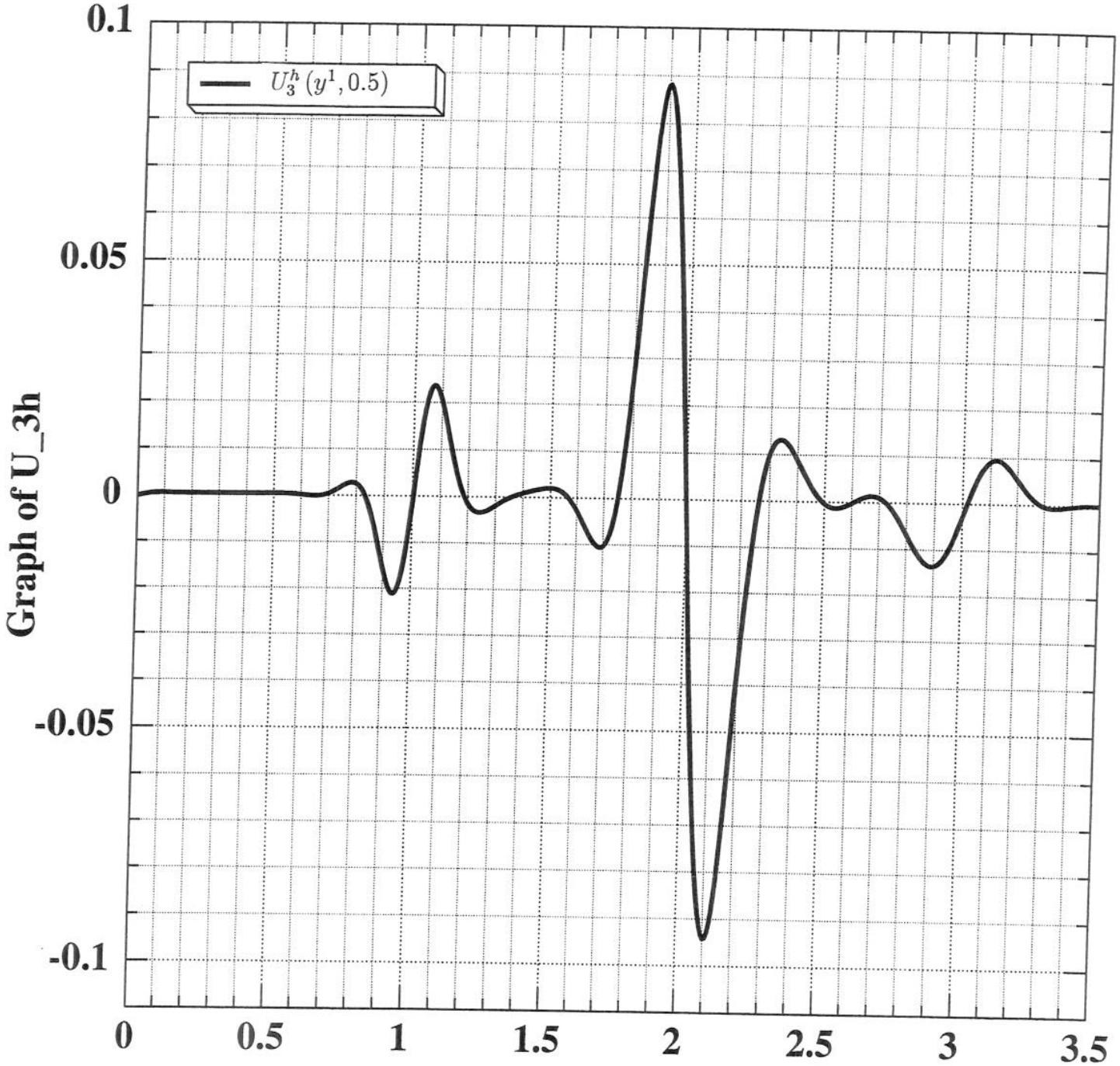

figure 4.3 : first example of loading, sect. 3.1. Plot of u_3 for $y^2 = 0.5$ exhibiting a propagated δ' - like singularity at $y^1 = 1$ and $y^1 = 2$.

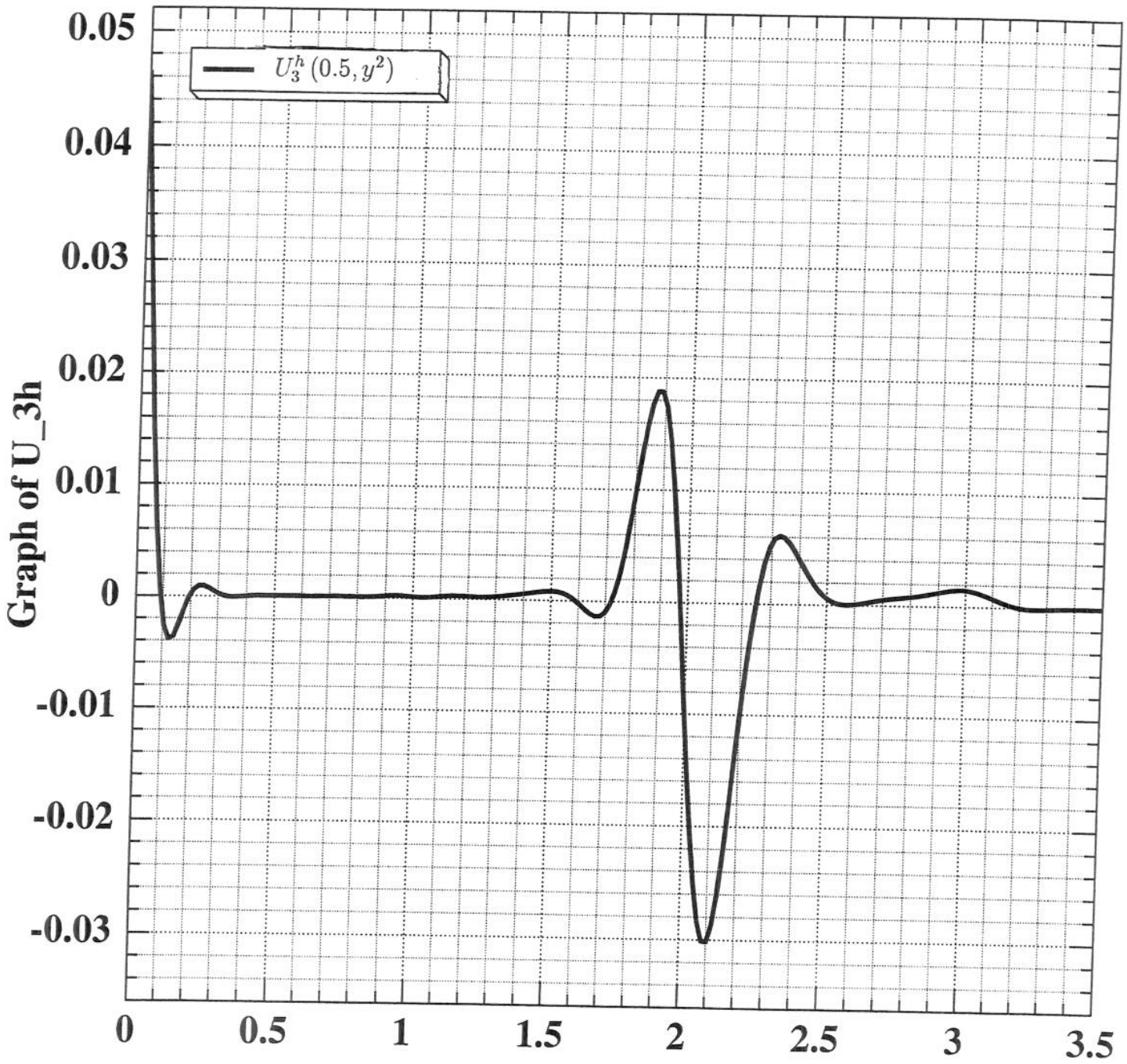

figure 4.4 : second example of loading, sect. 3.2. Plot of u_3 for $y^1 = 0.5$
exhibiting a propagated δ' - like singularity at $y^2 = 2$
and a propagated boundary layer at $y^2 = 0$.

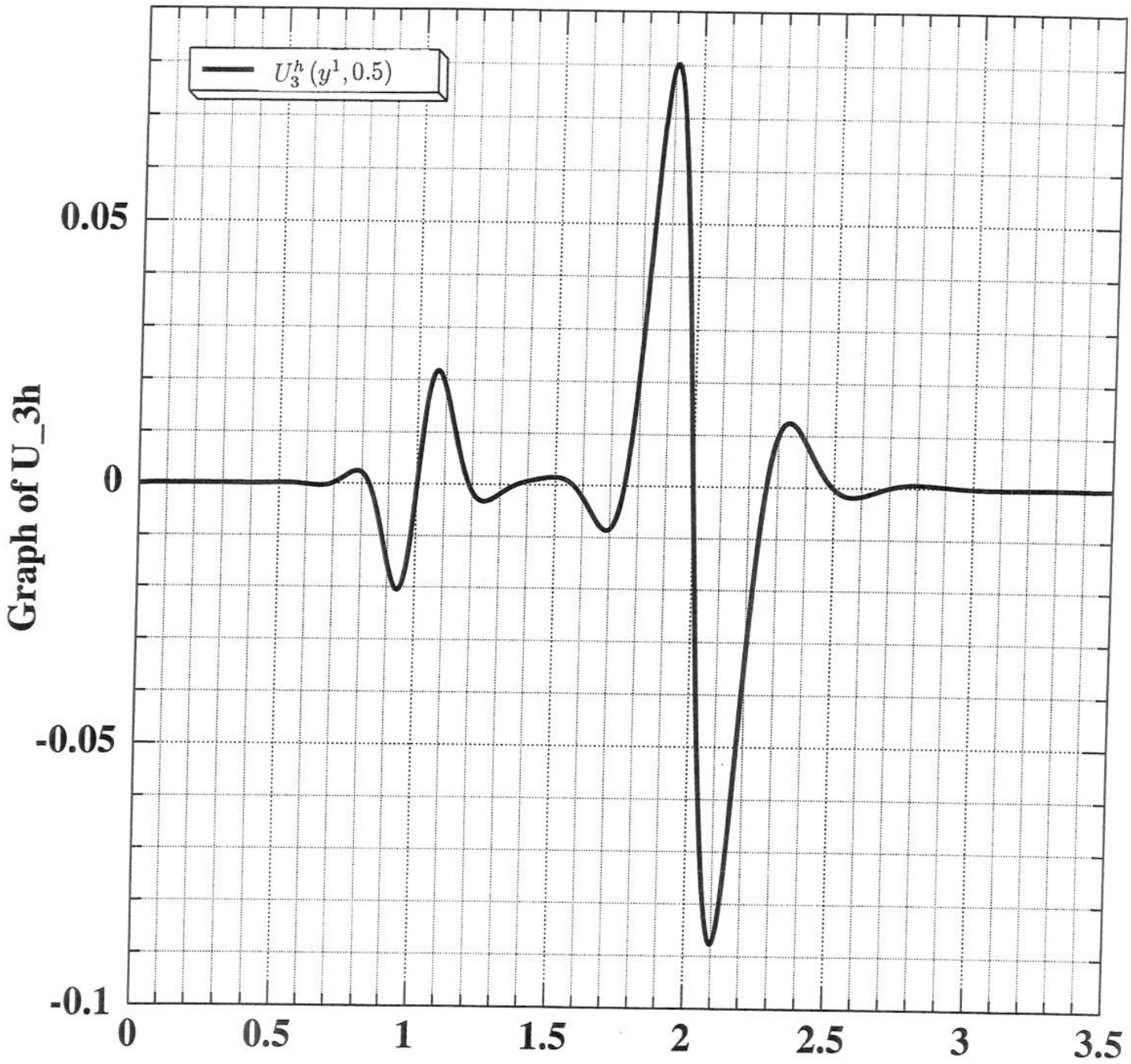

figure 4.5 : second example of loading, sect. 3.2. Plot of u_3 for $y^2 = 0.5$ exhibiting two propagated δ' - like singularities at $y^2 = 2$ and a ~~propagated boundary layer~~ at $y^2 = 0$.

Clamped hyperbolic shell

- $\Omega = \{(y^1,y^2) \in \mathbb{R}^2 | -L \leq y^1,y^2 \leq L\}$
- S is parameterized with the mapping (Ω,ψ)
- $\psi(y^1,y^2) = \left(y^1,y^2,\frac{y^1y^2}{c}\right)$
- Normal pressure (support A, B, C)

$$f^\alpha = 0$$
$$f^3 = 1$$

- ε between 10^{-3} and 10^{-5} to approach the limit problem solution

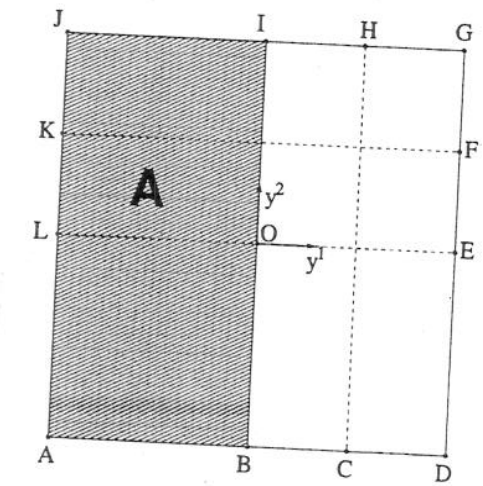

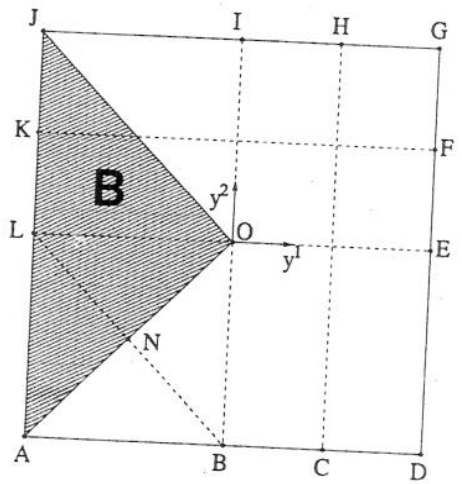

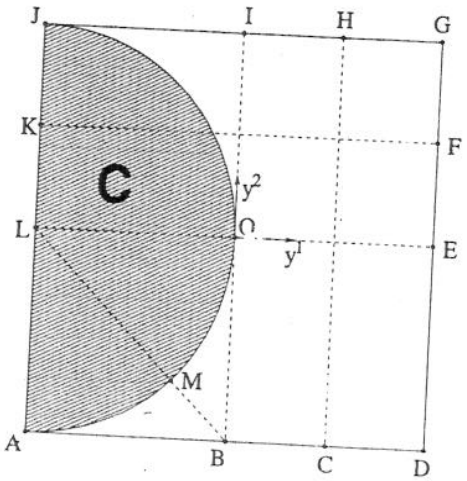

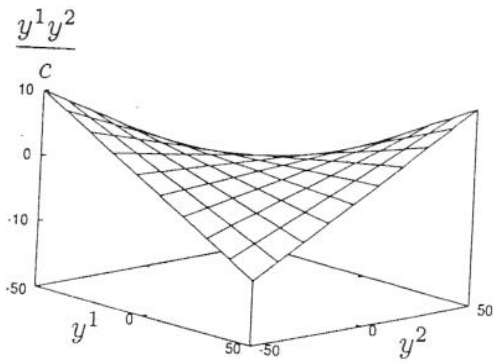

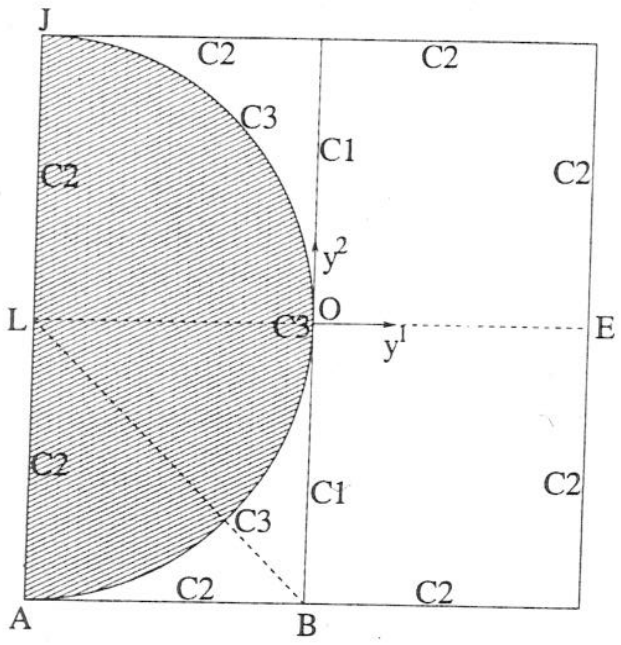

We consider $L = 50$ and $c = 250$. The material is isotropic and homogeneous, with Young modulus $E = 28500\,\text{MPa}$ and Poisson ratio $\nu = 0.4$. The values of the relative thickness ε are taken between 10^{-3} and 10^{-5}. The shell is clamped along the whole boundary. The coordinates curves $y^1 = const.$, $y^2 = const.$ are the asymptotic curves (characteristics) so that the coefficients $b_{\alpha\beta}$ of the second fundamental form are $b_{11} = b_{22} = 0, b_{12} \neq 0$. It should be noticed that the considered portion of surface is limited by asymptotic curves.

The loading is a uniform normal pressure on the regions A, B, C (the three cases shown in fig. which is taken to vary proportionally to the thickness.

Layer C1 - Singularities for the limit problem

Loading A

$$\begin{cases} u_1^0 = U_1(y^2)Y(-y^1) + \dots \\ u_2^0 = U_2(y^2)\delta(-y^1) + \dots \\ u_3^0 = U_3(y^2)\delta'(-y^1) + \dots \end{cases}$$

Loading B

$$\begin{cases} u_1^0 = U_1(y^2)y^1Y(-y^1) + \dots \\ u_2^0 = U_2(y^2)Y(-y^1) + \dots \\ u_3^0 = U_3(y^2)\delta(-y^1) + \dots \end{cases}$$

Loading C

$$\begin{cases} u_1^0 = U_1(y^2)(-y^1)^{1/2}Y(-y^1) + \dots \\ u_2^0 = U_2(y^2)\frac{-1}{2}(-y^1)^{-1/2}Y(-y^1) + \dots \\ u_3^0 = U_3(y^2)\frac{-1}{4}(-y^1)^{-3/2}Y(-y^1) + \dots \end{cases}$$

where Y, δ, δ' denote the Heaviside function, the Dirac mass and its derivatives, respectively, and $U_i(y^2)$ are smooth functions. It is understood that the terms denoted by dots are less singular than the previous ones at $y^1 = 0$.

Computations are carried out for various uniform and adapted meshes. The figure displays the meshes of a adaptation process with 5 iterations for $\varepsilon = 10^{-4}$ for the case of loading B.

The process starts with a coarse mesh and the adaptating code increases the number of nodes until 18091 nodes (49830 degrees of freedom). After the third iteration the adaptation process starts to

lengthen the finite elements in the layers (the limits of the loading, the propagation lines $y^1 = 0$ and $y^2 = 0$ and the boundary of the domain). The aspect ratio of the elements is the parameter used to measure this stretching. It gradually increases until the fifth iteration where the aspect ratio attains to 27.6.

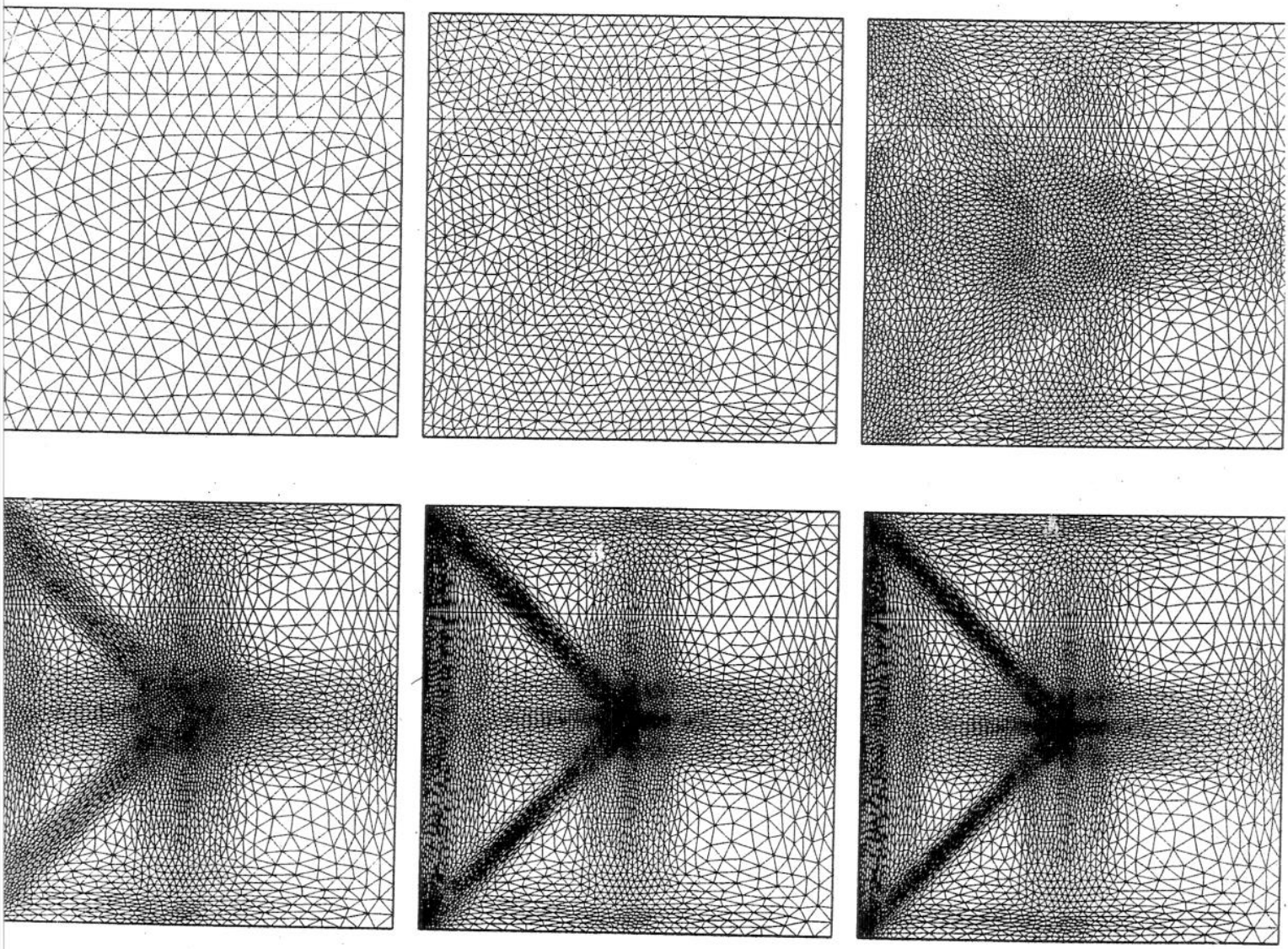

Adaptation process in the case of loading B - $\varepsilon = 10^{-4}$ - Iterations 0, 1, 2, 3, 4 and 5 with 1897, 5295, 11397, 16554, 17910 and 18091 nodes respectively.

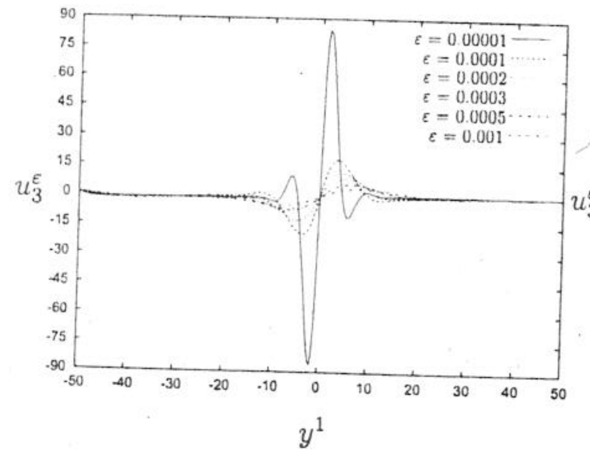

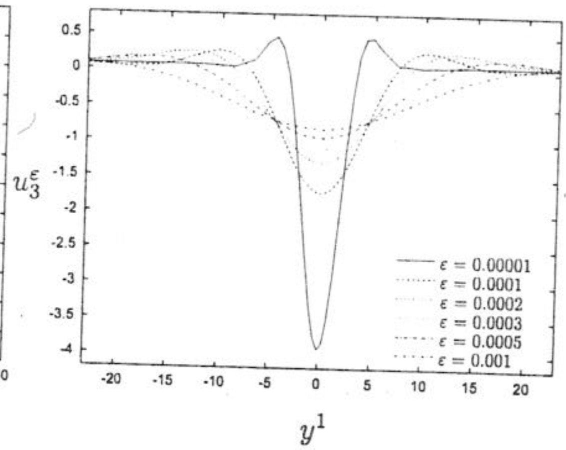

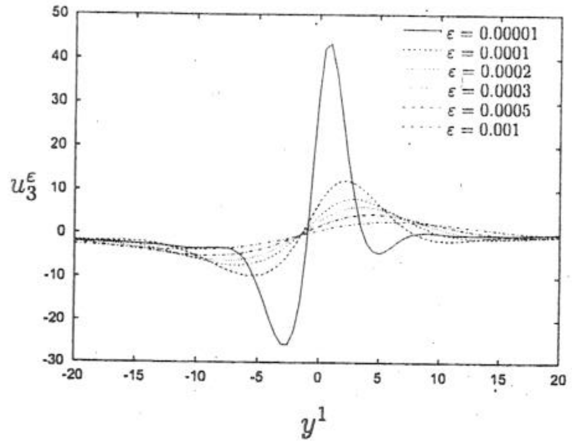

Cases of loading A, B and C -

Plot of u_3^ε for $y^2 = 0$

exhibiting propagated singularities

In the cases A and B it is apparent that as ε tends to zero, the solutions clearly converge to the δ and δ' foreseen singularities for the limit problem. In case C we have an intermediate situation, according to the theory. Clearly, for moderately small values of ε, the limit is not apparent: it only appears as a tendency.

Sketch to see that the singularity of f^3 in $y^1 = 0$ amounts to a jump of the first order derivative, of value $\delta(y^2)$

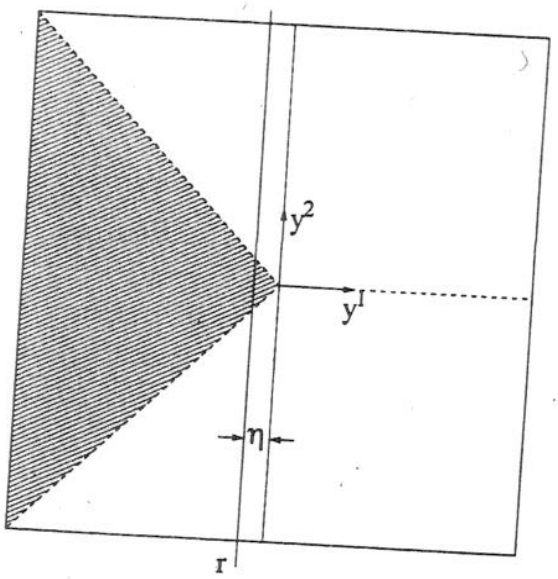

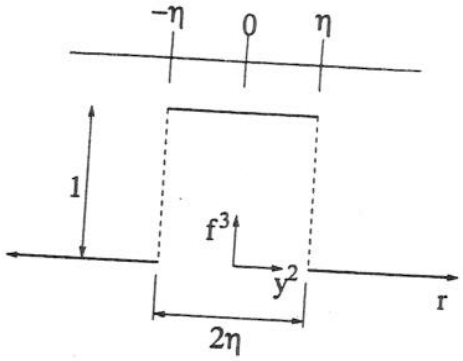

$$f^3 = \theta_{[-\eta,\eta]}(y^2)$$

$$f^3 = 2\eta\left(\frac{1}{2\eta}\theta_{[-\eta,\eta]}(y^2)\right)$$

Order of magnitude of u_3^ε on the layer C1

- Loading A - $u_3^\varepsilon = \mathcal{O}(\varepsilon^{-2/3})$
- Loading B - $u_3^\varepsilon = \mathcal{O}(\varepsilon^{-1/3})$
- Loading C - $u_3^\varepsilon = \mathcal{O}(\varepsilon^{-1/2})$

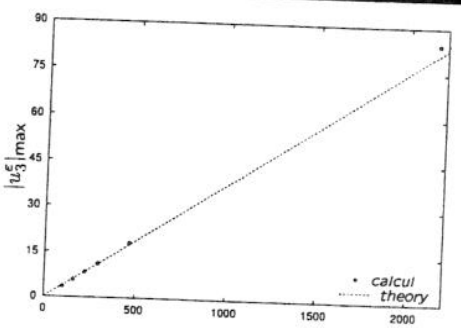

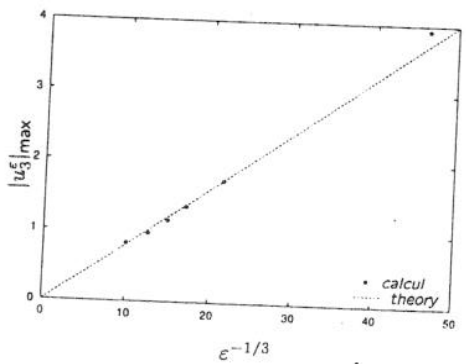

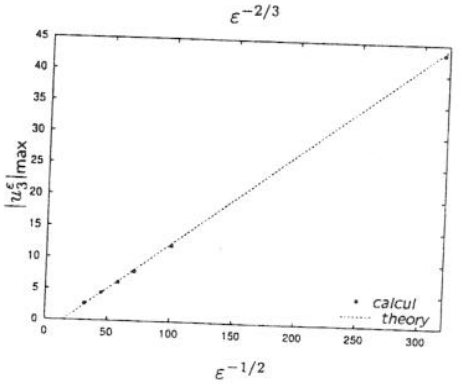

Order of magnitude of the boundary layer thickness

- Layer C1 on the asymptotic line
- $\eta_1 = \mathcal{O}(\varepsilon^{1/3})$?

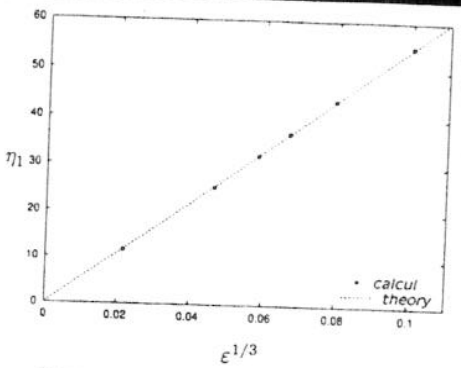

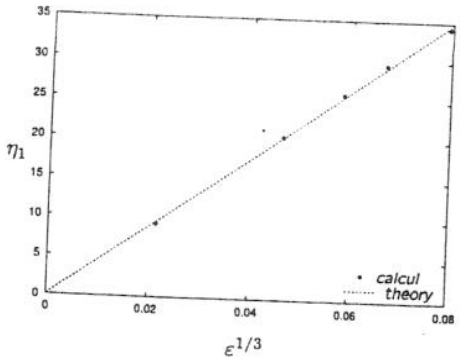

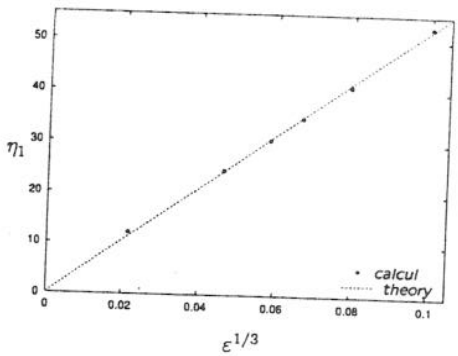

Layer C3 on the non-characteristic line

$$\eta_3 = \mathcal{O}(\varepsilon^{1/2}) \ ?$$

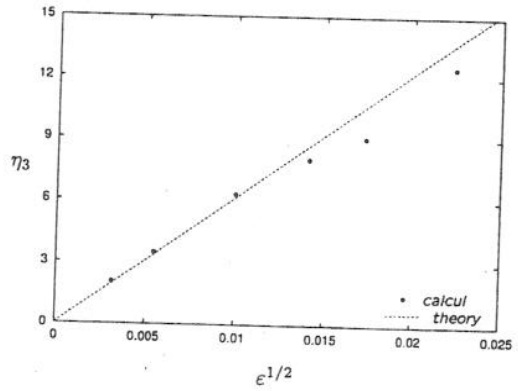

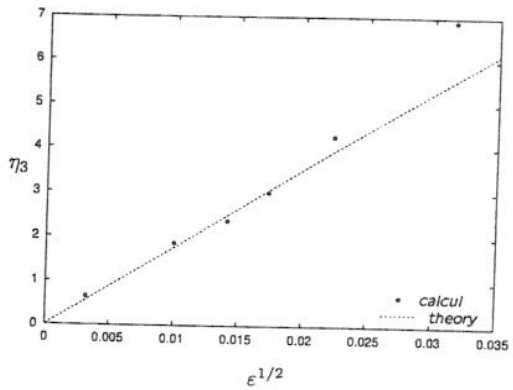

Conclusions

- Adapted mesh procedures leads to a significant advantage on more traditionnal mesh processors in terms of computation cost and accuracy.
- The method allows to detect the areas where refinements and anisotropic meshes are required.
- The advantage of the adaptation is much more relevant for small values of ε.
- Good estimation of the orders of magnitude of the boundary layer thickness.

PARABOLIC CASE (example: CYLINDER)

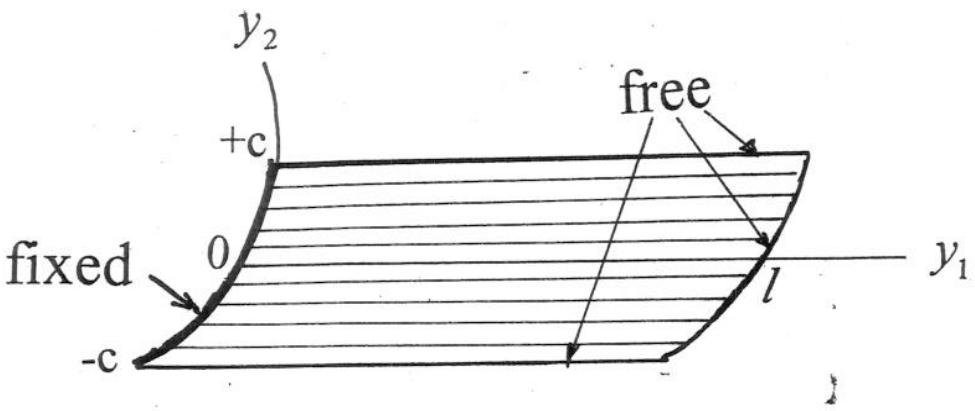

$$(3).....-\partial_1 T^{11} - \partial_2 T^{12} = 0$$

$$(2).....-\partial_1 T^{12} - \partial_2 T^{22} = 0$$

$$(1).....-b_{22} T^{22} = f^3$$

$$(4).....\partial u_1 = A_{1111} T^{11} + A_{1122} T^{22}$$

$$(5).....\frac{1}{2}(\partial_2 u_1 + \partial_1 u_2) = 2A_{1212} T^{12}$$

$$(6)\partial_2 u_2 - b_{22} u_3 = A_{2222} T^{22} + A_{1122} T^{11}$$

With (boundary conditions for u_3 does not make sense; boundary layer):

$$T^{11}(0, y_2) = T^{12}(l, y_2) = 0$$

$$u_1(0, y_2) = u_1(l, y_2) = 0$$

The system is uniquely solvable in the order 1 to 6. (Note that boundary conditions on $y_2 = +c$ and -c are not used, and in general not satisfied: boundary layers)

A very curious kind of solutions

Let $f^3 = \delta(y_2)F(y_1)$; then,

$$T^{22} = \delta(y_2)S^{22}(y_1)$$
$$T^{12} = \delta'(y_2)S^{12}(y_1)$$
$$T^{11} = \delta''(y_2)S^{11}(y_1)$$

$$u_1 = \delta''(y_2)U_1(y_1) + \delta(y_2)V_1(y_1)$$
$$u_2 = \delta'''(y_2)U_2(y_1) + \delta'(y_2)V_2(y_1)$$
$$u_3 = \delta^{(4)}(y_2)U_3(y_1) + \delta''(y_2)V_3(y_1) + \delta(y_2)W_3(y_1)$$

Where all the functions are well determinated.

For that loading, the membrane problem has a unique (distribution) solution. It is supported by the segment $y_2=0$ (but the problem is two-dimensional, involving ∂_2).

Intuitive picture (for small thickness η):

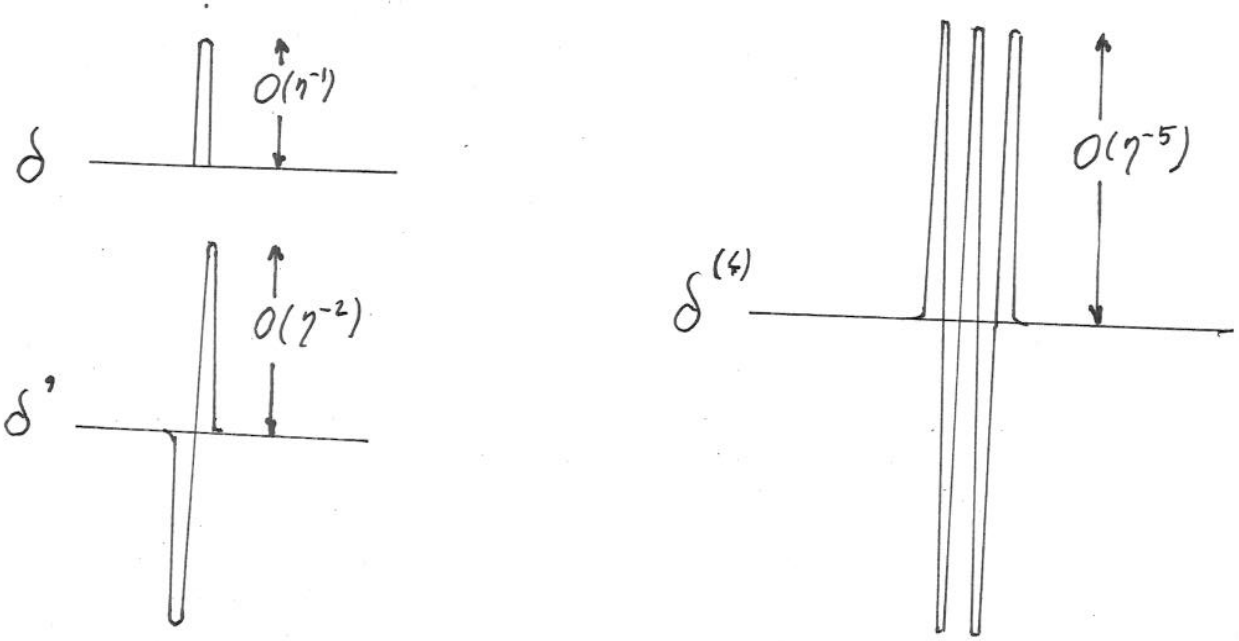

Obviously, the previous solution of the membrane problem does not make physical sense.

When considering the (small !) flexion terms, i. e. we take into account $\varepsilon > 0$, ($\varepsilon << 1$), u^{ε} has a boundary layer with thickness $0(\varepsilon^{1/4})$, which tends (in the distribution sense) to the membrane solution. It is exponentially decreasing out of the layer.

A "computational solution" for $\varepsilon = 10^{-3}$:

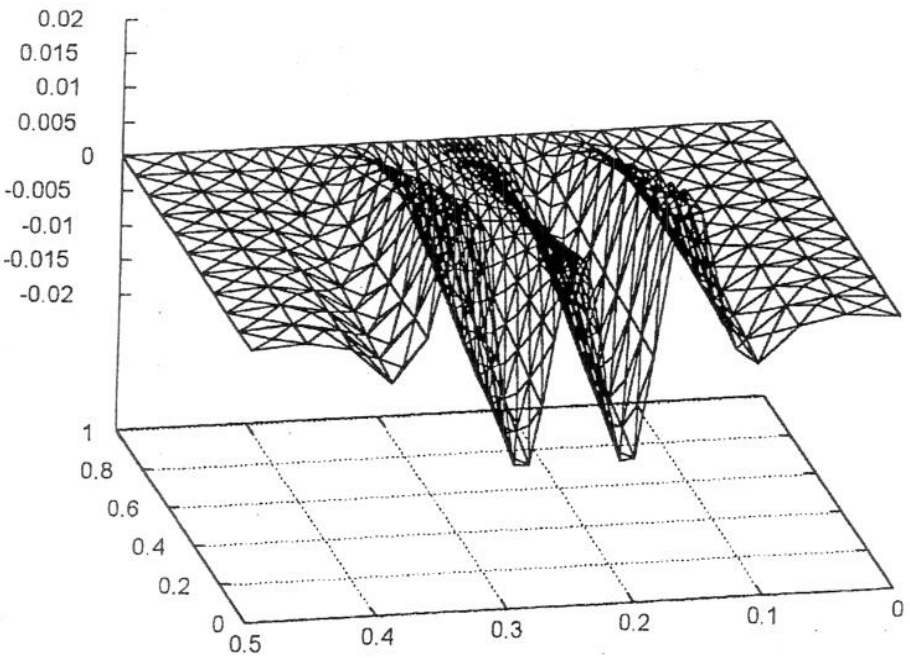

Plot of u_3^{ε} in the whole domain.

Analytic functionals and complexification

Distributions constitute a generalization of functions. They admit singularities of growing order, for instance:

$$\delta(x), \delta'(x), \delta''(x), \dots$$

But they are "of finite order" (i. e. on each bounded domain they are derivatives of finite order of continuous functions) . An expression of the form

$$u(x) = \sum_{k=1}^{+\infty} c_k \delta^{(k)}(x)$$

Is not a distribution, but an analytic functional (i. e. the test – functions are analytic, and in particular, localization properties are lost: analytic functionals have no support).

The corresponding Fourier Transforms have increasing growing at infinity:

$$1_\xi, i\xi, (i\xi)^2, \dots$$

Certain analytic functionals have Fourier Transforms which are distributions (and even functions) but with exponential growing at infinity (they are not "tempered distributions"). For instance,

$$\cosh(\xi) = \sum_{k=0}^{+\infty} \frac{\xi^{2k}}{(2k)!} \qquad \xi \in \mathbb{R}$$

Is the Fourier transform of the expression

$$u(x) = \sum_{k=0}^{+\infty} \frac{1}{(2k)!} (-i)^{2k} \delta^{(2k)}(x)$$

Which, as we know, is not a distribution. In fact, Fourier transform is a tool to deal with infinite order singularities.

Before going on with our singular perturbation problem, let us see an example of a sequence of (classical) functions converging to an analytical functional.

Let us consider approximation by truncation of the Fourier transform to the frequencies $\xi < \lambda$, and let λ tend to infinity. For instance:

$$\hat{f}(\xi) = \cosh \xi = \sum_{n=0}^{+\infty} \frac{1}{(2n)!} \xi^{2n}$$

$$f(x) = \delta(x) - \frac{\delta''(x)}{4!} + \frac{\delta^{(4)}(x)}{8!} - \ldots$$

and the approximant functions are

$$f^{\lambda}(x) = \frac{1}{2\pi} \int_{-\lambda}^{+\lambda} \cosh(\xi) \cos(\xi x) d\xi$$

$$\frac{1}{2\pi(x^2+1)} \left\{ e^{\lambda} \left[\cos(\lambda x) + x sin(\lambda x) \right] - e^{-\lambda} \left[\cos(\lambda x) - x sin(\lambda x \right. \right.$$

As we are interested in $\lambda \nearrow +\infty$, we shall discard the term in $e^{-\lambda}$, so that

$$f^{\lambda}(x) \approx \frac{e^{\lambda}}{2\pi} \psi^{\lambda}(x)$$

with

$$\psi^{\lambda}(x) = \frac{1}{x^2+1} \left(\cos(\lambda x) + x \sin(\lambda x) \right)$$

We then observe that the inverse Fourier transforms involve *two* scales, x and λx. This is a complexification phenomenon which does not appear when approaching Fourier transforms with algebraic growing (i.e. tempered distributions, the inverse Fourier transform of which is a *distribution*):

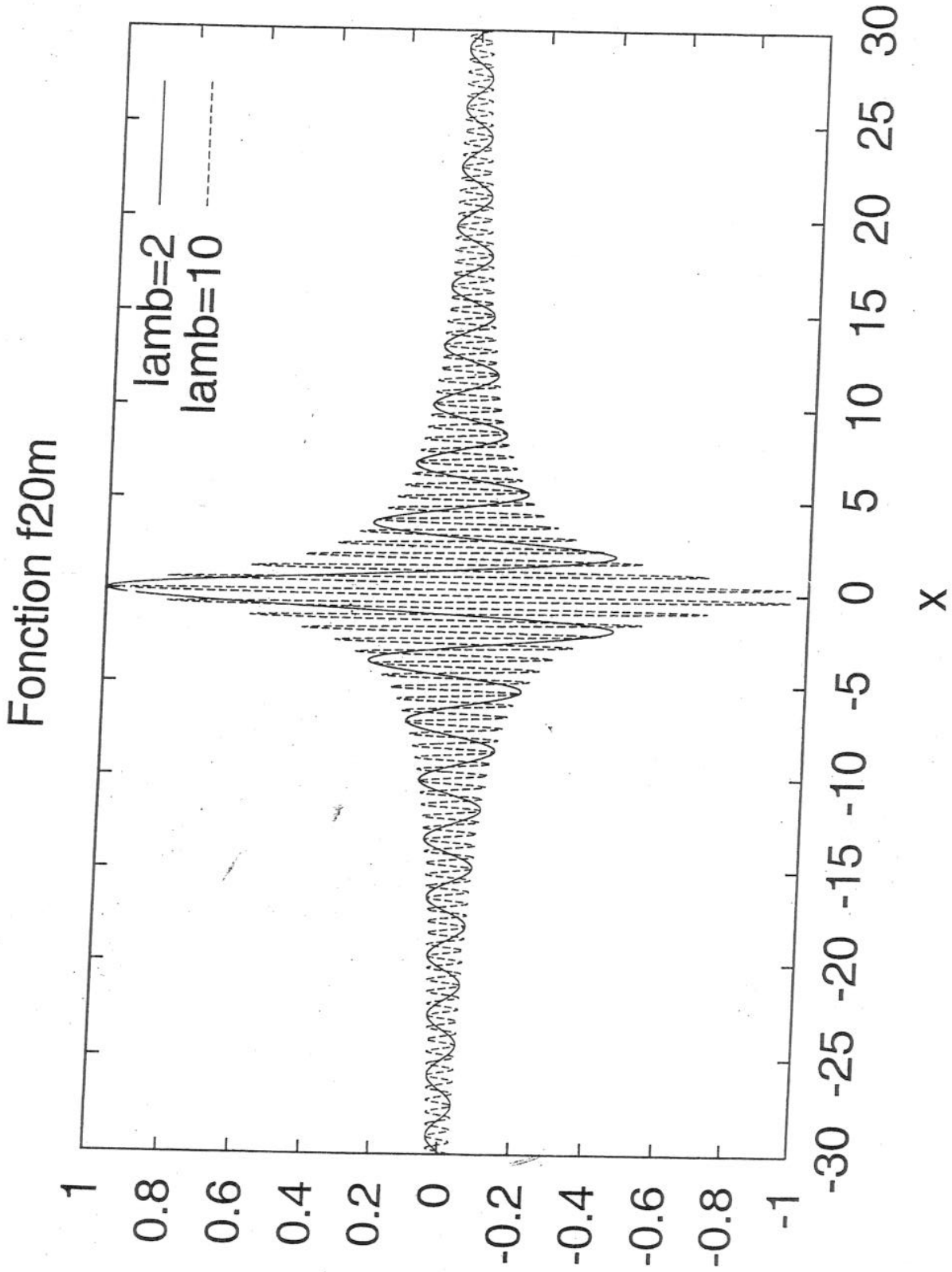

FIG. 1 – Fonction $f^{\lambda}(x) = \frac{cos(\lambda x)+xsin(\lambda x)}{x^2+1}$ pour $\lambda = 2$ et $\lambda = 10$

In fact, the solution of the limit problem is exponentially growing for ξ tending to infinity, but with fixed (small) ε, the solution ~~is~~ decays algebraically with a factor ε^{-2}. This implies the ***emergence of a new (moderately large)*** parameter $\log(\varepsilon^{-1})$ describing the characteristic frequency of the transition region, which is responsible for the lea di~~l~~g part of the solution for small ε.

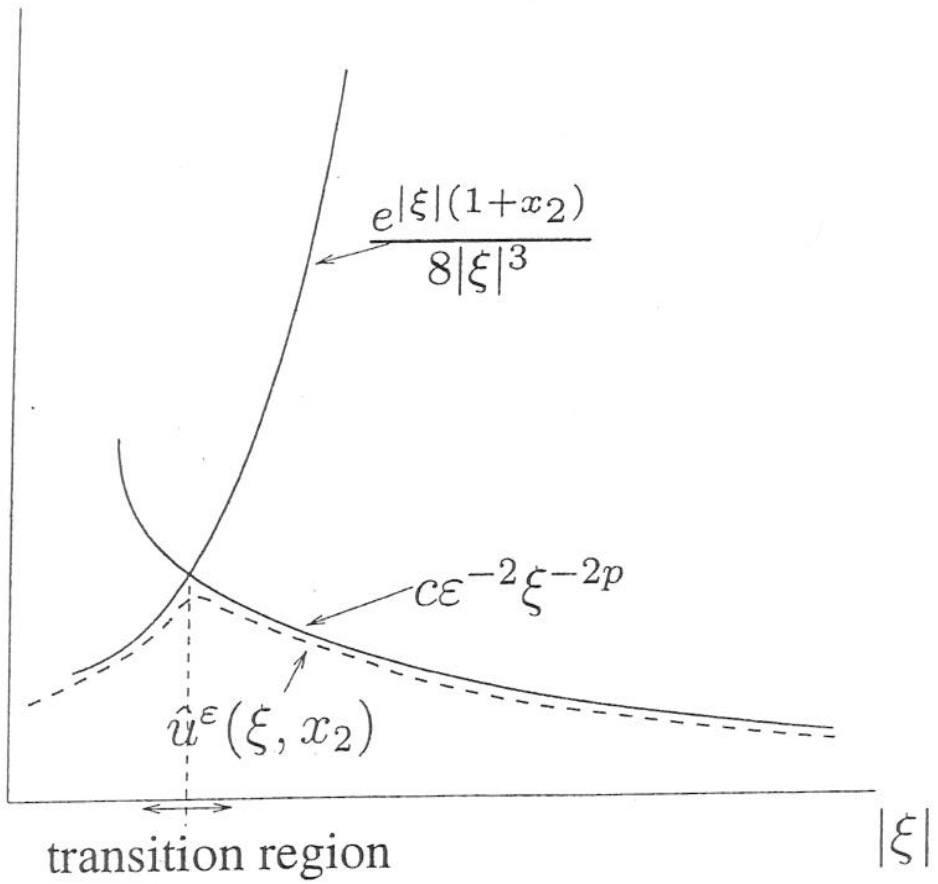

Figure 5. $\hat{u}^\varepsilon(\xi, x_2)$ for fixed $\varepsilon > 0$

CONVERGENCE OF THE FOURIER TRANSFORMS

Plot of $u_{\varepsilon}^{\wedge}(\xi,1)$. They converge as $\varepsilon \to 0$ in the distribution sense to a function with exponential growing for $|\xi| \to \infty$:

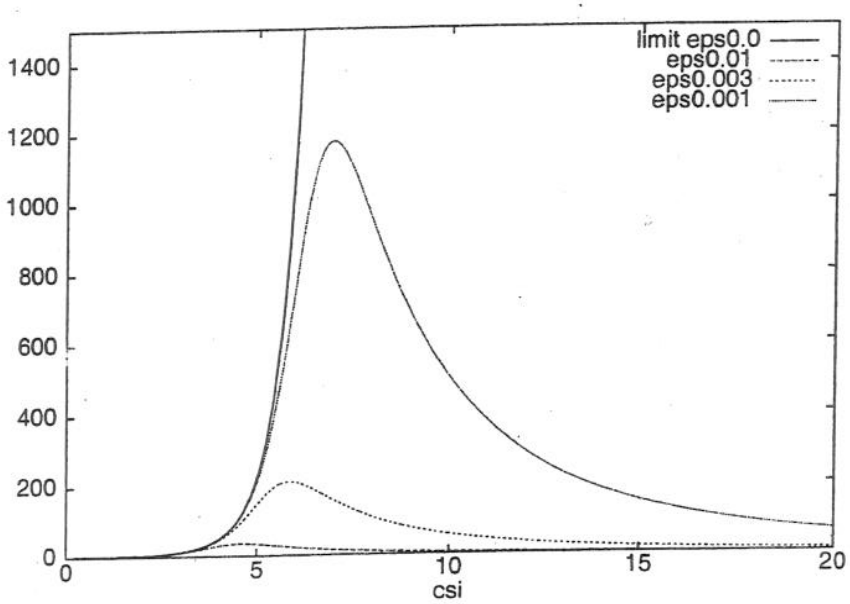

Exemple of an elliptic paraboloïd

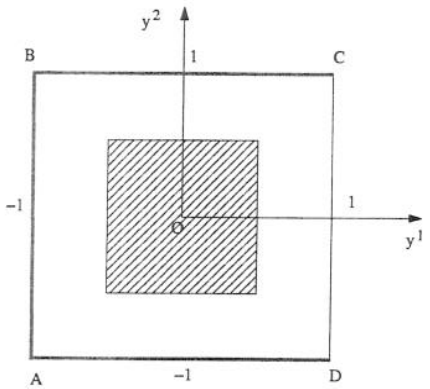

$$\vec{\psi}(y^1, y^2) = \left(y^1, y^2, (y^1)^2 + (y^2)^2\right)$$

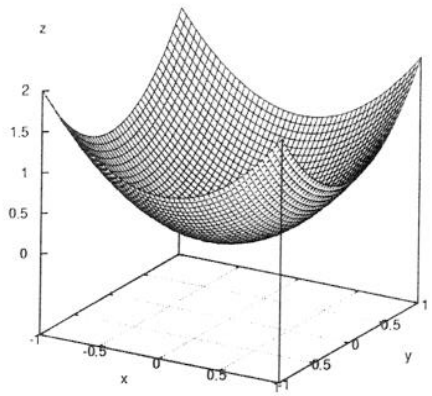

- Loading $f^3 = -10\epsilon$ applied in the loading domain (hatched square)
- Boundary conditions :
  - Clamped on AB, BC and AD
  - Free or clamped on CD

Well-inhibited case : *the edge CD is clamped*

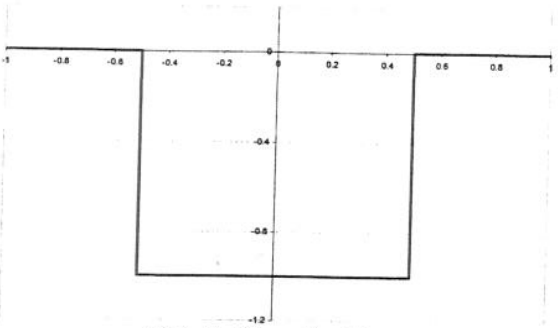

$f^3\ (y^1)$ (for $y^2=0$)

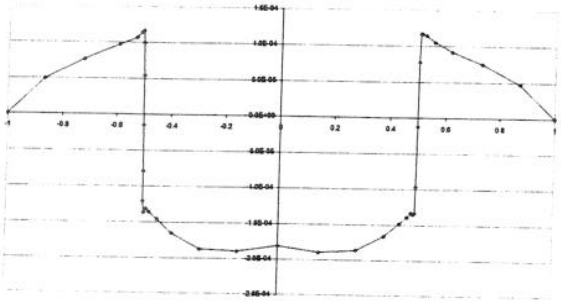

$u_3\ (y^1)$ (for $y^2=0$ and $\epsilon=10^{-5}$)

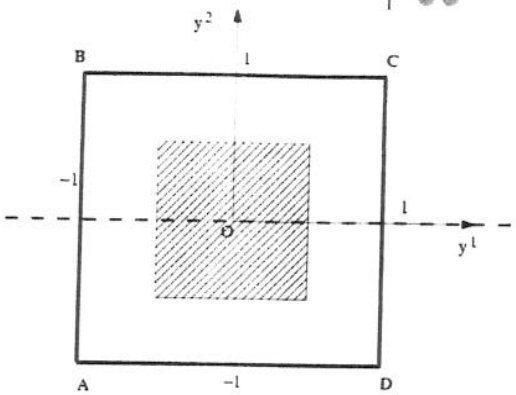

View on the line $y^2=0$

u_3 has the same singularites as f^3 as predicted by the theory

Logarithmic point singularity

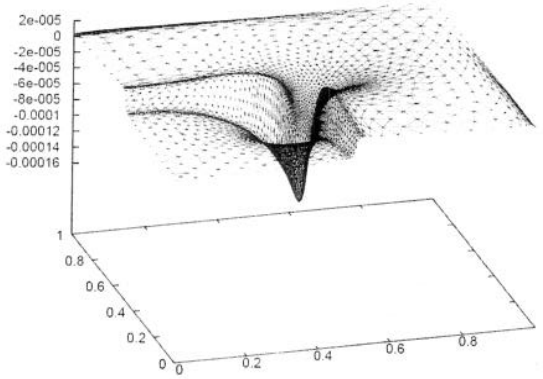

u_3 on a ¼ of the domain for $\epsilon=10^{-5}$

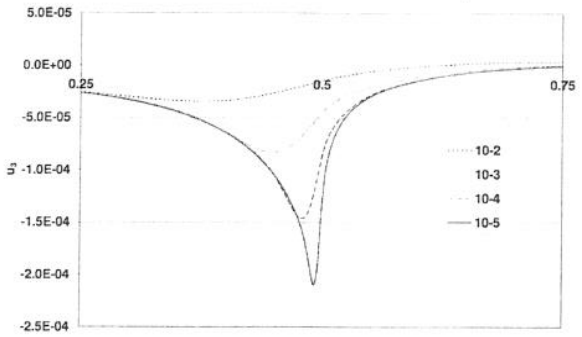

u_3 on the line $y^1=y^2$

➡ Existence of a logarithmic point singularity

- If the loading domain has a corner
- If the principal curvatures are diffrent at this point

(F. Béchet, E. Sanchez-Palencia, O. Millet : Computing singular perturbations for linear elliptic shells, *to appear in Computational Mechanics*, 2007)

Adaptive anisotropic mesh

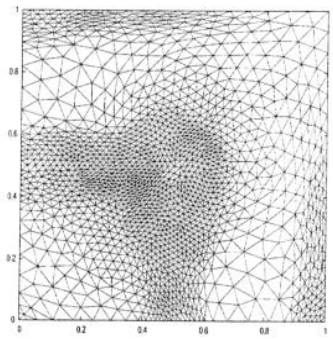

Third iteration (3076 elements)

Zoom of the mesh

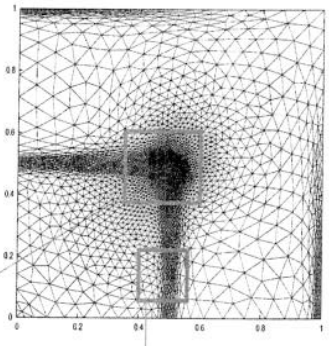

7th iteration (5351 elements)

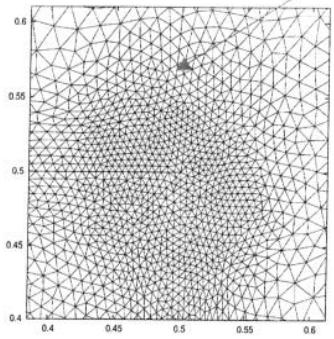

Isotropic mesh around the corner

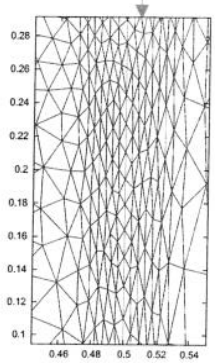

Anisotropic mesh in the layer

Necessity of an adaptive mesh procedure

Sensitive case

the edge CD is free

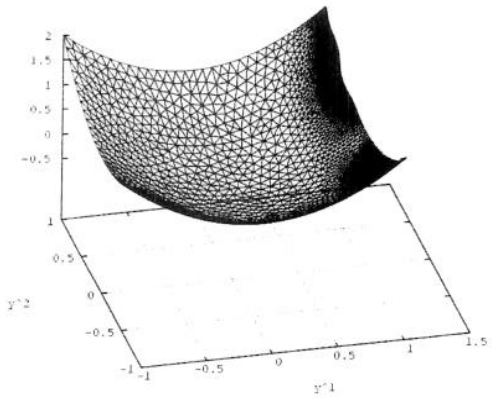

Deformed shape for $\epsilon=10^{-4}$

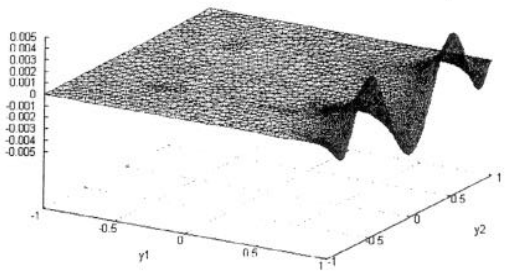

Displacement u_3 for $\epsilon=10^{-4}$

- The Shapiro-Lopatinskii condition is not satisfied
- Large oscillations along the free edge

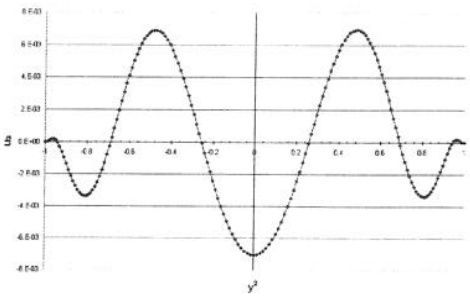

Displacement u_3 for $y^1=1$ and $\epsilon=10^{-4}$

Sensitive case

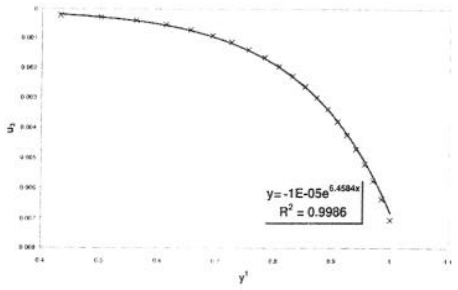

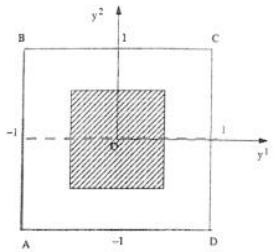

⇨ Oscillations exponential decreasing towards the interior of the domain

- Comparison with the well-inhibited case

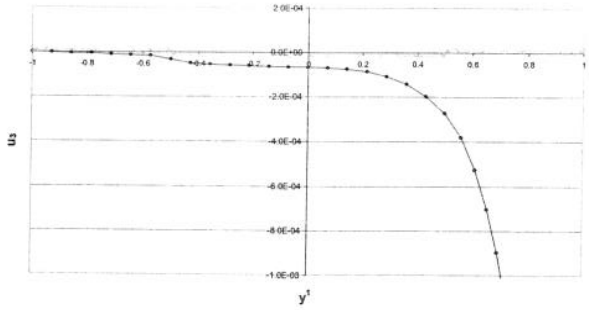

u_3 on the line $y^2=0$

- The singularities presented in the well-inhibited case are still present
- They are hidden by the large instability appearing near the free edge

Loss of rigidity of the shell as soon as a part of the boundary if free

Evolution of the oscillations on the free edge

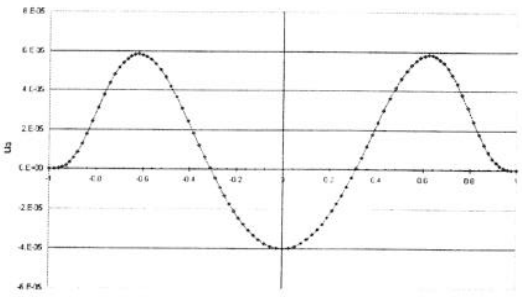

Displacement u_3 for $\epsilon=10^{-2}$

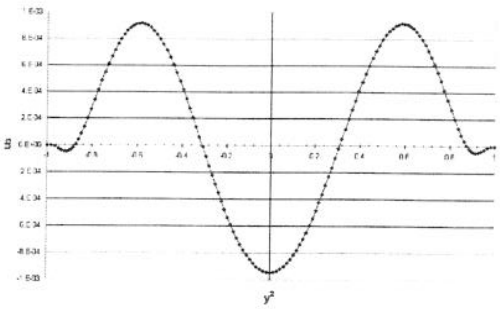

Displacement u_3 for $\epsilon=10^{-3}$

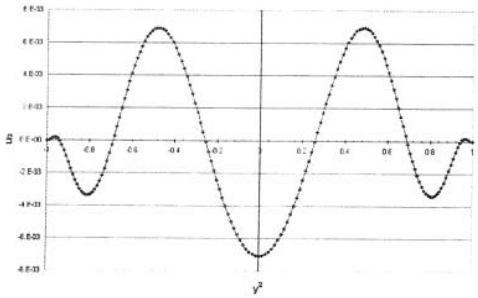

Displacement u_3 for $\epsilon=10^{-4}$

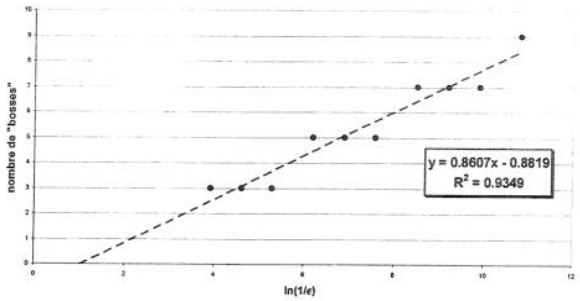

Number of oscillations vs $ln(1/\epsilon)$

➡ The number of oscillations varies like $ln(1/\epsilon)$

Membrane and bending energy

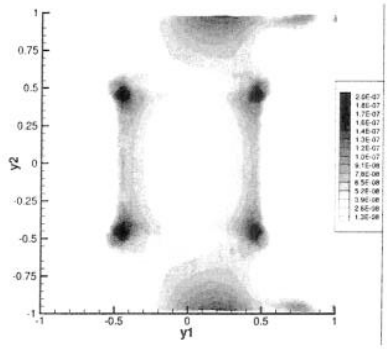

Membrane energy

Repartition of surface density of energies for $\epsilon=10^{-4}$

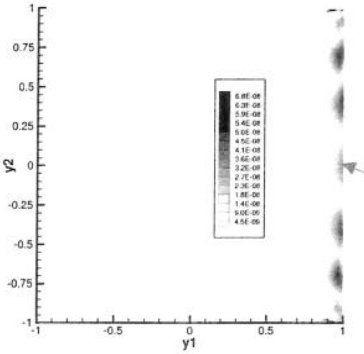

Benging energy

Free edge

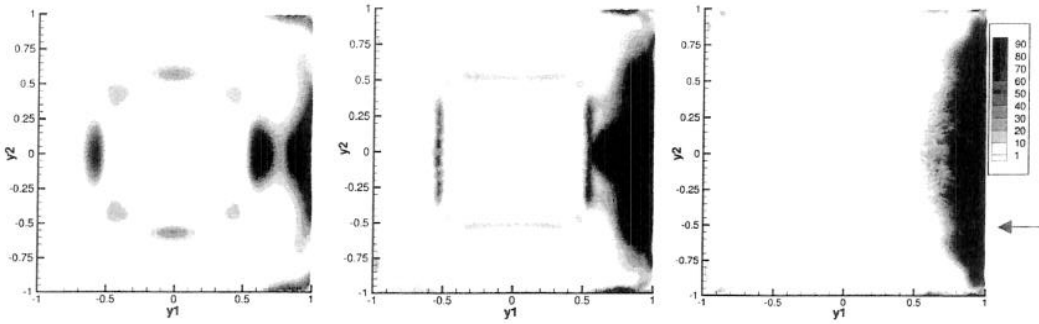

Percentage of bending energy for $\epsilon=10^{-2}$, $\epsilon=10^{-3}$ *and* $\epsilon=10^{-4}$